Proceedings of the ASME 2015 International Manufacturing Science and Engineering Conference
MSEC2015
June 8-12, 2015, Charlotte, North Carolina, USA

MSEC2015-9352

NEEDLE INSERTION FORCE MODEL FOR HAPTIC SIMULATION

Adam Gordon
Dept. of Mechanical Engineering
The Pennsylvania State University
University Park, PA, USA

Inki Kim
Dept. of Industrial Engineering
The Pennsylvania State University
University Park, PA, USA

Andrew C. Barnett
Dept. of Mechanical Engineering
The Pennsylvania State University
University Park, PA, USA

Jason Z. Moore
Dept. of Mechanical Engineering
The Pennsylvania State University
University Park, PA, USA

KEYWORDS
Needle Insertion, Tissue Cutting

ABSTRACT
Percutaneous medical procedures rely upon clinicians performing precise needle insertion in soft tissue. The utility of haptic simulation systems in training clinicians for these procedures is highly dependent upon the ability to render accurate insertion force feedback. This paper presents a piecewise mathematical model for insertion force that does not require tissue material properties, detailed mechanical approximations, or complex computations. With manipulation of model parameters, a wide variety of insertion tasks and clinical scenarios can be modeled. Through needle insertion experiments and parameter estimation, this model was demonstrated to replicate the insertion forces associated with a variety of needle and tissue types. In 11 of 12 needle and tissue combinations tested, the model replicated the insertion force with an average absolute mean error of less than 0.065 N.

INTRODUCTION
Central Venous Catheter insertions are performed over 5 million times per year in the United States [1]. While these procedures deliver essential medical care, mechanical complications, including arterial puncture, hematoma, and pneumothorax, have been reported at rates ranging from 5% to 21%. [1-3]. The occurrence of such complications has been correlated directly to clinician experience and training methodology, highlighting the need for medical simulation technology [2, 3]. In addition to Central Venous Catheter insertions, many percutaneous procedures exist that rely upon accurate placement of surgical needles, including tissue biopsy, brachytherapy, ablation, and lumbar puncture [4, 5]. Given that physicians rely heavily upon haptic perception to guide these needle insertions, accurate force feedback is a key element in computer based simulation systems [6]. To provide this feedback, a model for needle insertion force into soft tissues is required.

Modeling the force interactions during needle insertion into biological tissue has been a focus not just for medical simulation, but also for robotic surgery and preoperative planning [7]. Finite Element Methods (FEM) have been the focus of many works for modeling needle insertions and resulting tissue deformations. A common strategy has been to create a mesh framework representative of tissue, some works also adding a distinct mesh for the needle, with needle interaction forces simulated by boundary conditions applied to appropriate nodes [8-12]. Recent studies have also explored using advanced forms of FEM to more accurately simulate the needle insertion fracture mechanisms [13, 14]. Although it is a common simulation technique, there are major challenges associated with FEM. First, implementing accurate tissue constitutive equations is extremely difficult, as real tissue exhibits nonlinear and viscoelastic behavior [15]. While some models have incorporated a form of nonlinearity or viscoelasticity [13, 16-18], many instead approximate the tissue as linear elastic material [8-10, 14]. Due to large material deformations in certain clinical scenarios, these approximations are not always appropriate [17]. Second, FEM techniques for needle insertion have been widely acknowledged to have costly computational demand, sometimes inhibiting real-time simulation. For this reason, a significant focus of recent research has been on improving the computational efficiency of these methods [16, 18-20]. Lastly, model accuracy in FEM requires accurate estimation of tissue mechanical properties. These

estimations are challenging due to patient variability, biological variation in testing conditions, and tissue inhomogeneity [21, 22]. Many FEM models simplify this problem by assuming homogenous properties for regions of the same tissue type [10-14]. This comes at the expense of losing some of the inherent variability in insertion forces, such as those caused by anatomical substructures like vasculature, which have been shown to cause large peaks in insertion force [23].

In addition to FEM, there is a range of other models developed for needle insertion forces, several of which were developed with the potential to be implemented alongside FEM. A key model cited in many works divides the needle force into three sub-forces applied in a piecewise fashion: tissue stiffness, friction, and cutting. Stiffness force is modeled according to a second order polynomial, friction force is modeled by a Karnopp model, and cutting force is a constant [7]. In a similar model, this was extended to multiple layers of tissue with function parameters specific to each layer [24]. Within the realm of these schemes, the modeling of friction sub-force has been its own concentration of recent research [25, 26]. A notable limitation in this three force method is the absence of collisions with small internal structures that lie within a tissue layer and may influence insertion force [7].

To simplify the relationship between needle penetration depth and force, Hookean spring models have been another common theme in insertion force modeling. To simulate the needle passing through different tissue types, the spring constant varies for each tissue layer. Transitions between layers may be incorporated with empirical modifications to the overall force [27-29]. In some models, a linear viscous damping is also substituted for the fat layers. It is important to once again note that Hookean relationships are accurate for tissue only if small deformations occur in each layer, which is not always the case in a clinical situation [29]. In a more advanced form of the above layer modeling, a series of Voigt elements is used to capture some of these nonlinearities [30].

Online estimation in combination with a parameterized needle insertion model is a more complex method of mathematically modeling forces. In one instance, parameters were used that varied with time. This is impractical for force simulation applications, as parameters will have more data points associated with them than an original force data set [31]. Similar work utilized steady state convergence parameter values [4]. Another mathematical approach used a radial basis function network to form a non-linear approximation of insertion force [32]. Both of these approaches have yet to be demonstrated on real, inhomogeneous tissue.

In systems with advanced graphic renderings, insertion forces have been simulated using proxy-based algorithms. In general, proxies are assigned based upon the positions of graphical objects in the simulation, and the simulated needle tip position is virtually coupled to a proxy using a damper-spring combination. The force within this coupling dictates the force output of the simulation, and when it exceeds a given threshold, surfaces, such as an organ capsule, may be penetrated [33]. Parameter constants are assigned to each proxy coupling based upon the material properties of the graphical object interacting with the needle [34].

Other studies have focused on modeling the distribution of force over the length of the needle, with total insertion force coming from the integration of this distribution. The parameterization of these distributions is also dependent on approximating individual tissue as linear elastic material with uniform properties [35, 36].

In this paper, a modeling system for needle insertion force simulation is presented in which forces are parameterized according to a piecewise mathematical function. Through parameter manipulation, this model can replicate axial insertion force as a function of needle depth for a variety of insertion tasks. Within a given task, this manipulation also enables simulation of the high clinical variability in forces, which has been identified as a crucial element in clinician training [37]. Unlike the common existing models, this method, combined with a simple parameter fitting scheme, does not rely upon complex computation, determination of material properties, or detailed mechanical approximations.

Through a series of needle insertion experiments, the applicability of this model to several tissue types and needle geometries will be demonstrated and analyzed. First, the model function and the associated parameter fitting algorithm will be described. Second, the experimental procedure for measuring insertion forces and obtaining model parameters will be outlined. Third, the ability of the model to replicate the experimentally measured forces will be analyzed and discussed. Finally, conclusions from this work and directions of future study will be presented.

TISSUE INSERTION FORCE MODEL

Overview of Model

The model presented in this paper estimates the axial force acting on a needle as a function of the needle's insertion depth along a one dimensional path. In many insertions, the observed insertion force changes rapidly in a discontinuous fashion as various anatomical structures are being cut or punctured. The patterns of these discontinuities may vary considerably from one insertion to the next, even in the same tissue samples. Often, these discontinuities, such as non-linear peaks in force, can serve as critical haptic cues in the clinical setting [31, 37]. In order to capture the overall discontinuous and non-linear nature of needle insertion forces, an exponential function is applied in a piecewise manner over the length of an entire needle insertion task to obtain needle insertion force:

$$F(x) = \begin{cases} A_1 e^{B_1(x-D_1)} + C_1 & if\ 0 \le x < P_1 \\ A_2 e^{B_2(x-D_2)} + C_2 & if\ P_1 \le x < P_2 \\ \vdots & \\ A_n e^{B_n(x-D_n)} + C_n & if\ P_{n-1} \le x < P_n \end{cases} \quad (1)$$

Here, F is the insertion force as a function of needle insertion depth x, where x is zero when the needle first contacts tissue. A_n, B_n, C_n, and D_n parameterize the force at each piecewise segment n. The critical depth at which each piecewise phase terminates is denoted by P_n. In modeling force as a function of solely depth, the assumption of a constant, given insertion velocity is made for simplicity. Future work may study the velocity dependence of model parameters. In addition, the one dimensional nature of the model makes it appropriate only for simulations in which three dimensional needle manipulation for steering is not required.

Model Parameter Estimation

To obtain the model parameters for a real insertion task, a MATLAB based algorithm is implemented. As shown in Figure 1, this algorithm is highly effective in obtaining parameters for a variety of tissue types with starkly contrasting insertion force profiles. With measured force versus depth data input into the MATLAB program, a user is able to graphically segment the data into piecewise regions using data markers. These markers provide the initial set of P parameters. For this study, segmentation occurs wherever the global trend of the force has an abrupt discontinuity, as marked by red circles in Figure 1. With the data segmented, a non-linear least squares method is used to fit the exponential function individually to each phase. Next, the intersection positions of resulting phase functions are calculated using a built-in MATLAB solver. The critical depths, P_n, are then redefined as these intersection positions. This ensures that the overall force model does not have any abrupt jumps between piecewise phases. The final parameters for each phase are then output by the program and can be used to model the insertion force, as is done in Figure 1. Once markers are initially placed, the parameter estimation process typically takes less than 10 seconds on a standard PC.

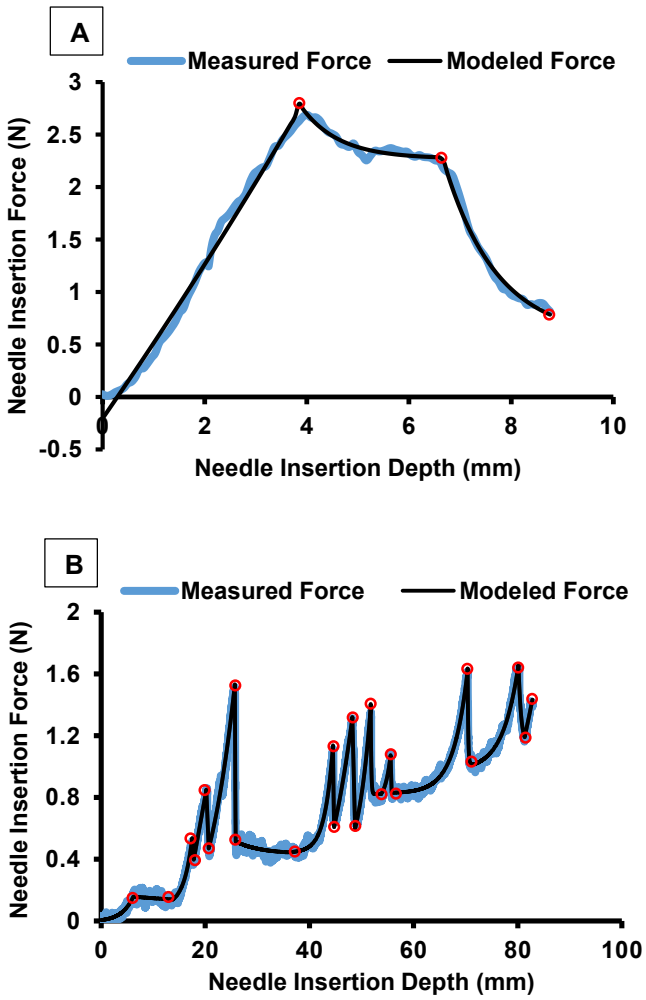

FIGURE 1—MEASURED INSERTION FORCE AND MODELED INSERTION FORCE FOR 18 GAUGE CONVENTIONAL HYPODERMIC INSERTION THROUGH PORCINE SKIN (A) AND 18 GAUGE BRACHYTHERAPY NEEDLE INSERTION INTO BOVINE LIVER (B); SEGMENTATION POINTS MARKED WITH RED CIRCLES

EXPERIMENTAL SETUP FOR FORCE MEASUREMENT AND PARAMETER ESTIMATION

Needle Insertion Experimental Setup

The laboratory setup shown in Figure 2 was utilized to acquire insertion force as a function of insertion depth in tissue samples. A linear actuator (Dunkermotoren) drove the needle into samples at a controlled constant velocity. To measure insertion force, a six-axis load cell (ATI) was coupled to the base of the needle. A LabView interface and data acquisition system (National Instruments, PXIe-6361) operated the actuator and recorded data.

Needle insertions were performed on four different tissue types: bovine liver, porcine skin, homogeneous phantom gel (M.F. Manufacturing Company), and a catheter insertion training mannequin (CAE Healthcare, BPH 660 Series). The phantom gel was made of polyvinyl chloride modified with plastisol and formulated with a 5:1 plastic to softener ratio. This gel has been commonly used as a soft tissue simulant for needle insertion experiments [38, 39]. The CAE Healthcare mannequin is a popular catheter insertion training tool that replicates relevant anatomical features, including an artificial artery and vein, surrounded by synthetic material. While the artificial tissues did not require any fixture for the insertion, specialized fixtures were employed to constrain the biological tissues. As shown in Figure 2, the bovine liver sample was placed in a plastic prism with slots on either side to allow needle insertion. To prevent movement within the prism, the top plate applied a constant pressure of 25 psi through a pneumatic pump. For the porcine skin, two aluminum plates clamped the tissue, allowing only local deformations in the regions of uniformly-distributed insertion holes.

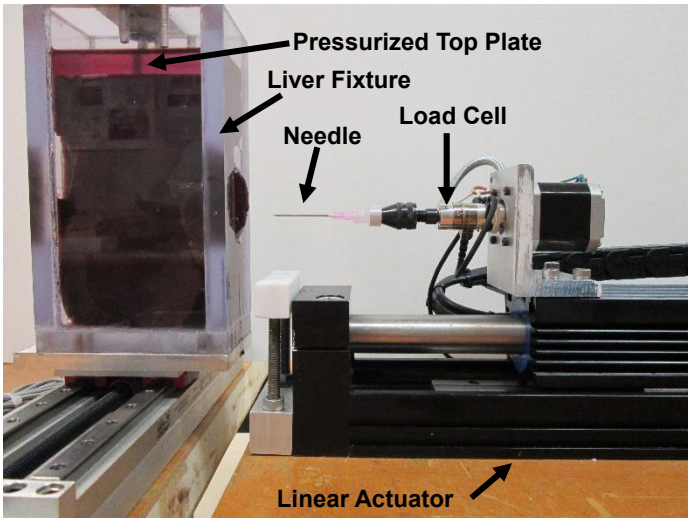

FIGURE 2—NEEDLE INSERTION FORCE MEASUREMENT SETUP WITH BOVINE LIVER FIXTURE

Experimental Design

The combinations of needles and tissues tested are shown in Table 1, with five trials performed for each combination. Insertion velocity was held constant across all tests at 8 mm/s, a velocity within the range for clinical procedures [40]. Images of the needles utilized in experiments and their bevel geometries are shown in Figure 3. Following experimentation, insertion force data sets were input into the MATLAB algorithm to obtain model parameters for individual trials. The mannequin was tested in two configurations: with and without an add-on layer that simulates patients with excess fat tissue.

TABLE 1—CLINICAL NEEDLES AND TISSUE TESTED

Needle	Clinical Use	Tissue Tested
18 Gauge Conventional Hypodermic	General Use	Bovine Liver, Porcine Skin, Mannequin W/ Fat, Mannequin No Fat, Phantom
18 Gauge Prostate Seeding Needle	Brachytherapy	
18 Gauge Catheter Hypodermic	Catheter Insertion	Mannequin W/ Fat, Mannequin No Fat

RESULTS AND DISCUSSION

Model Outcomes and Accuracy

The parameters found for each trial were applied to the insertion force model and used to obtain model-predicted force values at each depth for individual trials. The absolute mean error over the course of an entire insertion trial was obtained by comparing the modeled force with measured force at each depth. The absolute mean error of trials for the same insertion task were averaged for comparison, and are displayed by needle and tissue type in Figure 4. Experimentation shows that in all tissue and needle combinations, except the brachytherapy needle in porcine skin, the average error was below 0.065 N. The higher error of the brachytherapy needle in porcine skin is likely attributable to the much larger initial peak magnitude of force measured for the insertion, as can be seen in Figure 6. Similarly, the bovine liver, which saw the smallest insertion peak magnitudes, had the smallest average error for both needle types.

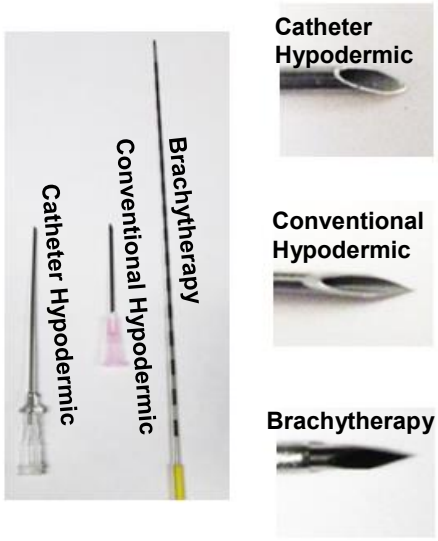

FIGURE 3—NEEDLES USED IN EXPERIMENTATION (LEFT) AND THEIR BEVELS (RIGHT)

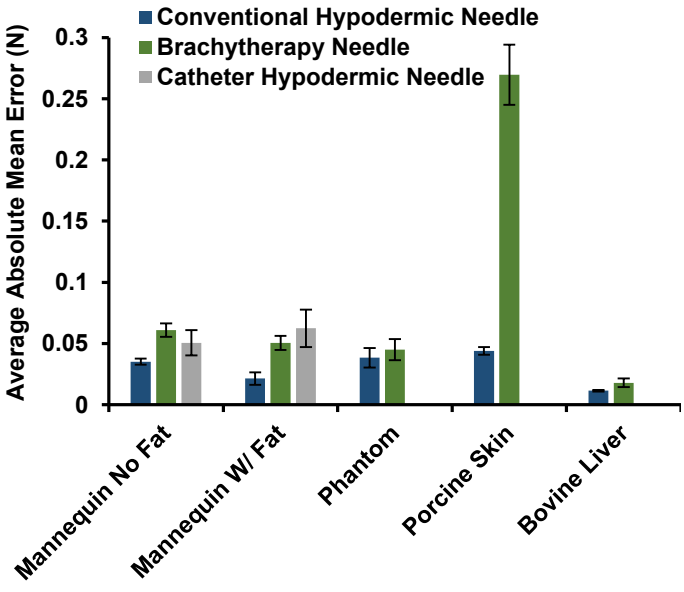

FIGURE 4—ABOLUTE MEAN ERROR FOR MODEL OVER ENTIRE INSERTION AVERAGED BY NEEDLE AND TISSUE TYPE; +/- 1 STANDARD DEVIATION AMONG TRIALS IS SHOWN BY ERROR BARS

The sample model outputs shown in Figures 5, 6, and 7 demonstrate the ability of the model to capture key differences between insertions in different tissues. For needles going through homogeneous tissue, the insertion force is continuous overall and is modeled in only one or two phases. However, for needles going through inhomogeneous tissue, the insertion force is highly discontinuous and is modeled in several phases. When the conventional hypodermic and brachytherapy needles were inserted into the phantom or the mannequin without fat, the tissue encountered was homogeneous. There was no initial force peak for these tissues due to the minimal force required to initially puncture the tissue. In these cases, the force rises in a near linear fashion as friction increases with insertion depth due to the additional contact area. When the brachytherapy and conventional hypodermic needles were inserted into the porcine skin, bovine liver, and mannequin with fat, the tissue encountered by the needle was inhomogeneous. This was also the case when the catheter hypodermic needle was inserted into the mannequin with and without fat, as without fat, the catheter needle was positioned such that it punctured the mannequin's artificial artery. In these inhomogeneous tissue insertions, rapid, discontinuous transitions in the force were observed. For example, when a layer of excess fat was added to the mannequin, a transition point occurred when the needle exited the fat layer and entered the normal mannequin. This transition can clearly be seen with all three needles around an insertion depth between 15 and 20 mm. For the liver insertions, many peaks can be observed which correspond to the needle puncturing through the variety of internal structures within the organ, such as vasculature and connective tissue. In porcine skin insertion, a rapid build-up of force occurs as the needle strains the tissue prior to puncturing through, resulting in a rapid release of force.

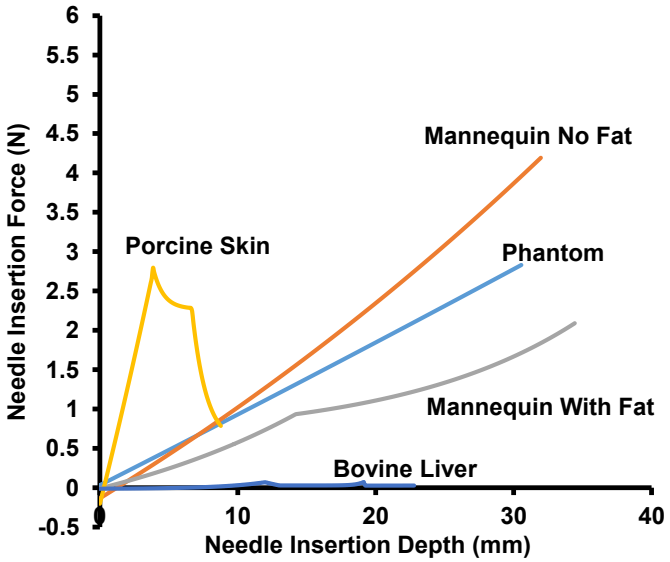

FIGURE 5—SAMPLE MODEL OUTPUTS FOR CONVENTIONAL HYPODERMIC NEEDLE

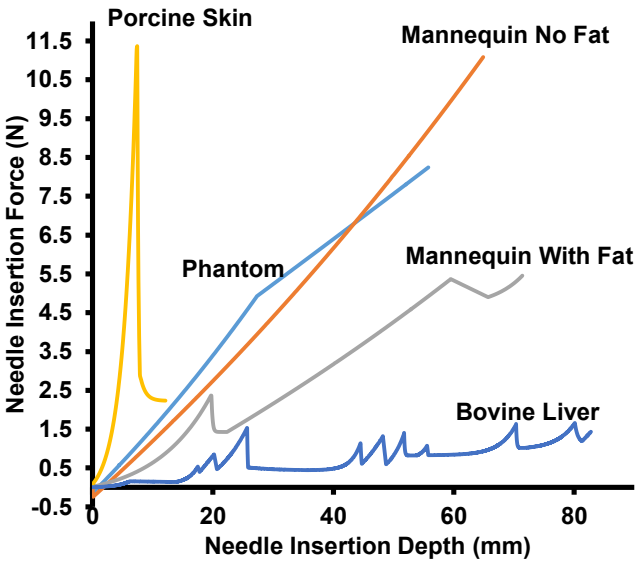

FIGURE 6—SAMPLE MODEL OUTPUTS FOR BRACHYTHERAPY NEEDLE

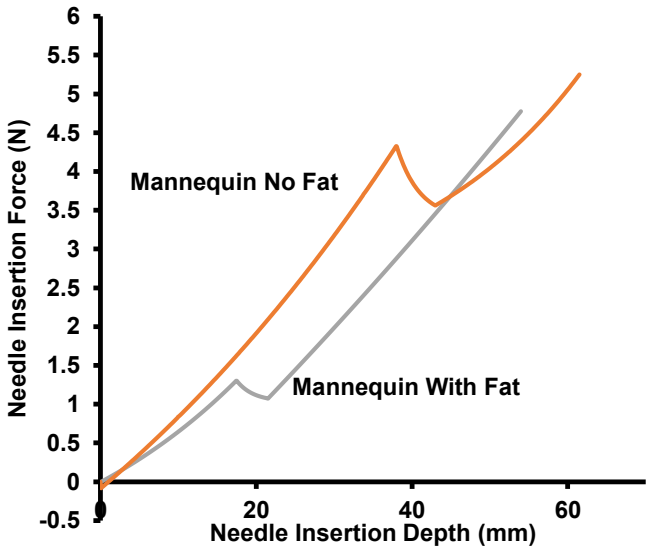

FIGURE 7—SAMPLE MODEL OUTPUTS FOR CATHETER HYPODERMIC NEEDLE

The model outputs also demonstrate the ability of the model to capture key differences in insertion force associated with different needle geometries. For example, the brachytherapy needle through porcine skin has a single rise and a single release of force. However, the conventional hypodermic needle through porcine skin has a single rise followed by two distinct releases. The conventional hypodermic has a longer bevel that results in the initial force release when the bevel first enters the tissue, then the second release once the entire bevel has pierced through the tissue. However, the brachytherapy needle bevel's shorter length and duller tip require a greater strain in the tissue prior to

puncture. This results in a greater initial force build up that precedes only a single, rapid release of force. The difference between the insertions with these two needles is captured in the model by adding an additional piecewise phase for the conventional hypodermic needle and modifying parameters within phases to enable the greater peak force observed with the brachytherapy needle.

Analysis of Error

Error was plotted as a function of insertion depth for each trial, as shown in Figure 8, to gain insight into the model accuracy beyond the absolute mean error values. In phantom and mannequin insertions for the brachytherapy and conventional hypodermic needles, one of the largest contributions to model error occurred at the beginning of the insertion. In fact, in some cases, this even resulted in a small negative force to be initially predicted by the model. A likely cause for this error was that in the measured data, the insertion force rose initially in a very non-linear fashion due to initial deflection of tissue. As friction became the dominant force, the force rise took on a more linear form. There was no abrupt discontinuity between these behaviors, thus only one piecewise phase was assigned to them. This resulted in model error at the very beginning of the insertion where the force was briefly more non-linear. In future modeling, this could be addressed by assigning a separate phase to the initial non-linear portion, despite there being no abrupt discontinuity.

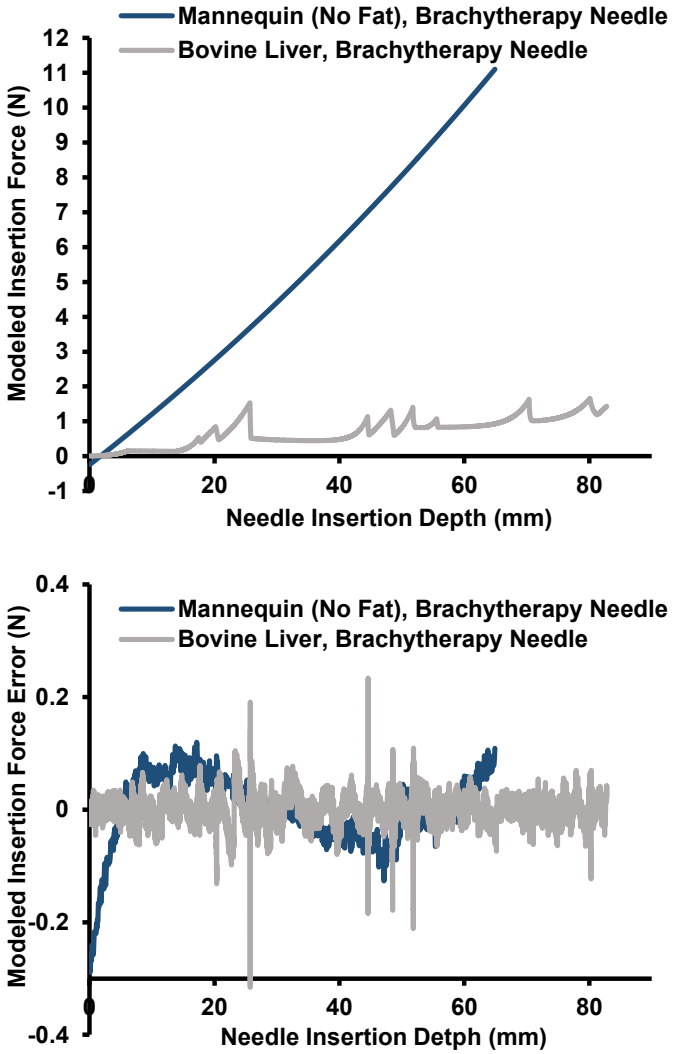

FIGURE 8—SAMPLE INSERTION MODEL FOR INDIVIDUAL TRIALS AND CORRESPONDING ERROR PLOTS

In comparing the bovine liver error plot of Figure 8 with its corresponding model, it can be seen that major error spikes correspond to the large force peaks within the modeled data. The corresponding measured forces are shown in Figure 1B, where it can be visually observed that the model appears to predict the magnitude of these force peaks quite accurately. However, the position at which these peaks occur is shifted very slightly from the true position resulting in a brief significant error when the model is compared with the measured data. These miniscule shifts in position of the force peaks would likely have a negligible impact when it comes to using the model for haptic simulation.

The acceptable level of error in the force model is a question of the fidelity required in the overall simulation system. There is still significant debate as to what level of fidelity is truly necessary to provide effective medical training, particularly considering the cost trade-offs associated with attempting to increase fidelity [28]. In this model, error can be further reduced by segmenting measured force data into much smaller sections. However, in doing so, the utility of the parameterization scheme is lost. The key advantage of this model is that it provides a simple framework for a variety of clinical scenarios to capture and manipulate the major haptic cues that occur along the axis of a needle as it progresses on a one dimensional insertion path.

CONCLUSION AND FUTURE WORK

A dynamic model has been presented for modeling axial needle insertion force as a function of insertion depth without many of the drawbacks associated with the complexity of other methods. By manipulating parameters, this model can be applied to a variety of insertion tasks and clinical scenarios. This adaptability has been demonstrated by using the model to replicate measured insertion forces for several needle and tissue type combinations.

The future goal of this work is to implement this modeling scheme into a low cost, low fidelity simulation system that can be used in training multiple needle insertion procedures. Prior to doing so, the velocity dependence of model parameters must be studied and incorporated into the model to provide additional realism to simulations. In addition, experimental data will need to be obtained for true clinical insertion procedures in order to establish the proper parameter values.

REFERENCES

[1] McGee, D. C., and Gould, M. K., 2003, "Preventing Complications of Central Venous Catheterization," The New England Journal of Medicine, 348(12), pp. 1123-1133.

[2] Eisen, L. A., Narasimhan, M., Berger, J. S., Mayo, P. H., Rosen, M. J., and Schneider, R. F., 2006, "Mechanical Complications of Central Venous Catheters," Journal of Intensive Care Medicine, 21(1), pp. 40-46.

[3] Evans, L. V., Dodge, K. L., Shah, T. D., Kaplan, L. J., Siegel, M. D., Moore, C. L., Hamann, C. J., Lin, Z., and D'Onofrio, G., 2010, "Simulation Training in Central Venous Catheter Insertion: Improved Performance in Clinical Practice," Academic Medicine, 85(9), pp. 1462-1469.

[4] Asadian, A., Kermani, M. R., and Patel, R. V., 2012, "A Novel Force Modeling Scheme for Needle Insertion Using Multiple Kalman Filters," IEEE Transactions on Instrumentation and Measurement, 61 (2), pp. 429-438.

[5] Podder, T. K., Sherman, J., Messing, E. M., Rubens, D. J., Fuller, D., Strang, J. G., Brasacchio, R. A., and Yu, Y., 2006, "Needle Insertion Force Estimation Model using Procedure-Specific and Patient-specific Criteria," *Proceedings of the 28th IEEE EMBS International Conference*, IEEE, pp. 555-558.

[6] Roth-Monzon, E.L., Chellali, A., Dumas, C., and Cao, C.G.L., 2011, "Haptic sensitivity in needle insertion: the effects of training and visual aid," *Proceedings of the International Skills Conference*, EDP Sciences, pp. 250-253.

[7] Okamura, A. M., Simone, C., and O'Leary, M. D., 2004, "Force Modeling for Needle Insertion into Soft Tissue," IEEE Transactions on Biomedical Engineering, 51(10), pp. 1707-1716.

[8] Goksel, O., Sapchuk, K., and Salcudean, S.E., 2011, "Haptic Simulator for Prostate Brachytherapy with Simulated Needle and Probe Interaction," IEEE Transactions on Haptics, 4(3), pp. 188-198.

[9] DiMaio, S. P., and Salcudean, S. E., 2005, "Interactive Simulation of Needle Insertion Models," IEEE Transactions on Biomedical Engineering, 52(7), pp. 1167-1179.

[10] Jin, X., Gao, D., and Lei, Y., 2014, "Interactive Simulation of Surgical Needle Insertion Into Soft Tissue," 2012, *ASME 2012 5th Annual Dynamic Systems and Control Conference*, ASME, pp. 457-464.

[11] Chentanez, N., Alterovitz, R., Ritchie, D., Cho, L., Hauser, K. K., Goldberg, K., Shewchuk, J. R., and O'Brien, J. F., 2009, "Interactive Simulation of Surgical Needle Insertion and Steering," ACM Transactions on Graphics, 28(3), Article 88.

[12] Lei, Y., and Lian, B., 2014, "Modeling and Simulation of Flexible Needle Insertion Into Soft Tissue Using Modified Local Constraint Method," *Proceedings of the ASME 2014 International Manufacturing Science and Engineering Conference*, ASME.

[13] Yamaguchi, S., Tsutsui, K., Satake, K., Morikawa, S., Shirai, Y., and Tanaka, H. T., 2014, "Dynamic analysis of a needle insertion for soft materials: Arbitrary Lagrangian-Eulerian-based three-dimensional finite element analysis," Computers in Biology and Medicine, 53, pp. 42-47.

[14] Oldfield, M., Dini, D., Giordano, G., and Rodriguez Y Baena, F., 2013, "Detailed finite element modelling of deep needle insertions into a soft tissue phantom using a cohesive approach," Computer Methods in Biomechanics and Biomedical Engineering, 16(5), pp. 530-543.

[15] Misra, S., Ramesh, K. T., and Okamura, A. M., 2008, "Modeling of Tool-Tissue Interactions for Computer-Based Surgical Simulation: A Literature Review," Presence, 17(5), pp. 463-491.

[16] Jin, X., Joldes, G. R., Wittek, A., and Miller, K., 2013, "3D Algorithm for Simulation of Soft Tissue Cutting," Computational Biomechanics for Medicine: Models, Algorithms and Implementation, pp. 49-62.

[17] Kobayashi, Y., Onishi, A., Watanabe, H., Hoshi, T., Kawamura, K., Hashizume, M., and Fujie, M. G., 2010, "Development of an integrated needle insertion system with image guidance and deformation simulation," Computerized Medical Imaging and Graphics, 34(1), pp. 9-18.

[18] Patriciu, A., 2012, "CUDA accelerated simulation of needle insertions in deformable tissue," Journal of Physics: Conference Series, 385(1).

[19] Sedeh, R.S., Ahmadian, M. T., and Janabi-Sharifi, F., 2010, "Modeling, Simulation, and Optimal Initiation Planning for Needle Insertion Into the Liver," Journal of Biomechanical Engineering, 132(4).

[20] Xu, J., Wang, L., Wong, K. C. L., and Shi, P., 2010, "A Meshless Framework For Bevel-tip Flexible Needle Insertion Through Soft Tissue," *Proceedings of the 2010 3rd IEEE RAS & EMBS International Conference on Biomedical Robotics and Biomechatronics*, IEEE, pp. 753-758.

[21] Hoshi, T., Kobayashi, Y., and Fujie, M. G., 2009, "Method to Generate Distribution Maps of the Material Parameters of the Human Body Using Robotic and Dynamic Simulation Systems," *IEEE/SICE International Symposium on System Integration*, IEEE, pp. 60-66.

[22] Kobayashi, Y., Okamoto, J., and Fujie, M. G., 2005, "Physical Properties of the Liver and the Development of an Intelligent Manipulator for Needle Insertion," *Proceedings of the 2005 IEEE International Conference on Robotics and Automation*, IEEE, pp. 32-39.

[23] Elgezua, I., Song, S., Kobayashi, Y., and Fujie, M. G., 2013, "Event Classification in Percutaneous Treatments based on Needle Insertion Force Pattern Analysis," *2013 13th International Conference on Control, Automation, and Systems*, ICROS, pp. 288-293.

[24] Carra, A., and Avila-Vilchis, J. C., 2010, "Needle Insertion Modeling through Several Tissue Layers," *2010 2nd International Asia Conference on Informatics in Control, Automation and Robotics*, IEEE, pp. 237-240.

[25] Asadian, A., Patel, R. V., and Kermani, M. R., 2014, "Dynamics of Translational Friction in Needle-Tissue Interaction During Needle Insertion," Annals of Biomedical Engineering, 42(1), pp. 73-85.

[26] Kobayashi, Y., Sato, T., and Fujie, M. G., 2009, "Modeling of Friction Force based on Relative Velocity between Liver Tissue and Needle for Needle Insertion Simulation Plates

Needle," *31st Annual International Conference of the IEEE EMBS*, IEEE, pp. 5274-5278.
[27] Luboz, V., Zhang, Y., Johnson, S., Song, Y., Kilkenny, C., Hunt, C., Woolnough, H., Guediri, S., Zhai, J., Odetoyinbo, T., Littler, P., Fisher, A., Hughes, C., Chalmers, N., Kessel, D., Clough, P. J., Ward, J., Phillips, R., How, T., Bulpitt, A., John, N. W., Bello, F., and Gould, D., 2013, "ImaGiNe Seldinger: first simulator for Seldinger technique and angiography training," Computer Methods and Programs in Biomedicine, 111, pp. 419-434.
[28] Manoharan, V., Gerwen, D. V., and Dankelman, J., 2012, "Design and Validation of an Epidural Needle Insertion Simulator with Haptic Feedback for Training Resident Anaesthesiologists," *IEEE Haptics Symposium 2012*, IEEE, pp. 341-348.
[29] Xia, P., and Sourin, A., 2012, "Design and Implementation of a Haptics-based Virtual Venepuncture Simulation and Training System," *VRCAI 2012*, ACM, pp. 25-30.
[30] Brett, P. N., Parker, T. J., Harrison, A. J., Thomas, T. A., and Carr, A., 1997, "Simulation of resistance forces acting on surgical needles," Journal of Engineering in Medicine, 211(4), pp. 335-347.
[31] Barbe, L., Bayle, B., de Mathelin, M., and Gangi, A., 2007, "In Vivo Model Estimation and Haptic Characterization of Needle Insertions," The International Journal of Robotics Research, 26(11-12), pp. 1283-1301.
[32] Narayanan, M.S., Zhou, X., Garimella, S., Waz, W., Mendel, F., and Krovi, V. N., 2012, "Data Driven Development of Haptic Models for Needle Biopsy Phantoms," 2012, *ASME 2012 5th Annual Dynamic Systems and Control Conference*, ASME, pp. 419-427.
[33] Mastmeyer, A., Hecht, T., Fortmeier, D., and Handels, H., 2014, "Ray-casting based evaluation framework for haptic force feedback during percutaneous transhepatic catheter drainage punctures," International Journal of Computer Assisted Radiology and Surgery, 9(3), pp. 421-431.
[34] Färber, M., Hummel, F., Gerloff, C., and Handels, H., 2009, "Virtual Reality Simulator for the Training of Lumbar Punctures.," Methods of Information in Medicine, 48(5), pp. 493-501.
[35] Crouch, J. R., Schneider, C. M., Wainer, J., and Okamura, A. M., 2005, "A Velocity-Dependent Model for Needle Insertion in Soft Tissue," Medical Image Computing and Computer-Assisted Intervention, pp. 624-632.
[36] Dehghan, E., Wen, X., Zahiri-Azar, R., Marchal, M., and Salcudean, S. E., 2007, "Parameter Identification for a Needle-Tissue Interaction Model," *Proceedings of the 29th Annual International Conference of the IEEE EMBS*, IEEE, pp. 190-193.
[37] van Gerwen, D. J., Dankelman, J., and van den Dobbelsteen, J. J., 2014, "Measurement and Stochastic Modeling of Kidney Puncture Forces," Annals of Biomedical Engineering, 42(3), pp. 685-695.
[38] Moore, J. Z., and Shih, A. J., 2010, "Tissue Oblique Cutting Flow Angle and Needle Insertion Contact Length," Transactions of NAMRI / SME, 38, pp. 711-718.
[39] Podder, T. K., Clark, D. P., Fuller, D., Sherman, J., Ng, W. S., Liao, L., Rubens, D. J., Strang, J. G., Messing, E. M., Zhang, Y. D., and Yu, Y., 2005, "Effects of Velocity Modulation During Surgical Needle Insertion.," *Proceedings of the 2005 IEEE Engineering in Medicine and Biology 27th Annual Conference*, IEEE, pp. 5766-5770.
[40] Dimaio, S. P. and Salcudean, S. E., 2003, "Needle Insertion Modeling and Simulation," IEEE Transactions on Robotics and Automation, 19(5), pp. 864-875.